

Figure 3. Chemiluminescent β -Gal reporter assays with fiber-modified adenovirus vectors and mAb6E3. (A) Transfer efficiency into PC12 cells. The cells were lysed and assayed for β -Gal activity using a commercial kit. The left panel indicates the efficiency of gene transfer into PC12 cells with AdvZ3-FZ33 alone (FZ33), AdvZ3-FZ33 and control mlgG₁ (FZ33 + mlgG₁), and AdvZ3-FZ33 and mAb6E3 (FZ33 + mAb6E3). The right panel indicates the efficiency of gene transfer with AdvZ3-FdZ alone (FdZ), AdvZ3-FdZ and control mlgG₁ (FdZ + mlgG₁), and AdvZ3-FdZ and mAb6E3 (FdZ + mAb6E3). Each dot represents the mean \pm SD of the four experiments. (B) Transfer efficiency into C6 cells. In the same experiments with C6 cells, there were no increases in mAb6E3-targeted gene transfer efficacy mediated by AdvZ3-FZ33 or AdvZ3-FdZ.

to the manufacturer's instructions. Specifically stained protein bands were extracted from the gel, digested by trypsin, and analysed by μ MALDI-Qq-TOF MS/MS QSTAR Pulsar i (Applied Biosystems Japan Ltd, Tokyo, Japan).

Cloning and transfection of Rat Na,K-ATPase cDNAs

The cDNAs of rat Na,K-ATPase α 1-4 (pRc alpha 1-4) were provided by Dr Lingrel (University of Cincinnati, USA). Total RNA of rat Na,K-ATPase β 1-3 and γ a, b and c was isolated from the PC12 cells using RNeasy mini kits (Qiagen, Hilden, Germany) according to the manufacturer's instructions. The cDNA was synthesized by reverse transcriptase-PCR. The oligonucleotide primers used to examine gene expression were: rat Na,K-ATPase β 1 forward primer 5'-AGCAGACACCATGGCCCGCGAA-3', reverse primer 5'-GTGCTGTGATCAGCTCTTAACCTCAA-3'; rat Na,K-ATPase β 2 forward primer 5'-CGTGCTCCAAGATGGTC-ATCCAA-3', reverse primer 5'-GGAGCCTCAGGCTTTGT-

TGATTCGA-3'; rat Na,K-ATPase β 3 forward primer 5'-TTCCACTCGCCCATCATGACGAAGA-3', reverse primer 5'-GCCTACTCCTAGGCATGTGCTATGA-3'; rat Na,K-ATPase γ a forward primer 5'-GAAATGACAGAGCTGTCA-GCTAACCA-3'; rat Na,K-ATPase γ b forward primer 5'-TCAGCTAACCATGGTGGCAGTGCAG-3'; rat Na,K-ATPase γ c forward primer 5'-CCACCATGGACAGGTGGTACTTGGTGGC-3'; rat Na,K-ATPase γ a, b, and c reverse primer 5'-TCTTCGGTCACAGCTCATCTTCATG-3'. The resulting cDNA was ligated into the pTarget vector (Promega). Each cDNA was transfected into 293T cells using LipofectAMINE Plus reagent (Invitrogen) by incubating in OptiMEM medium (Gibco BRL) at 37°C for 48 h. The 293T cells transfected with each cDNA of Na,K-ATPase and the rat cell lines were suspended in staining medium [PBS, 2% FBS, 0.05% NaN₃, and 1 mg/ml propidium iodide (PI)] containing saturating amounts of mAb6E3 or mlgG₁ (MOPC-21; BD Pharmingen) as a control. The reactivity of cells with mAb6E3 and mlgG₁ was determined by flow cytometry using a FACS Calibur system. Dead cells defined by positive staining with PI were gated out from the analysis.

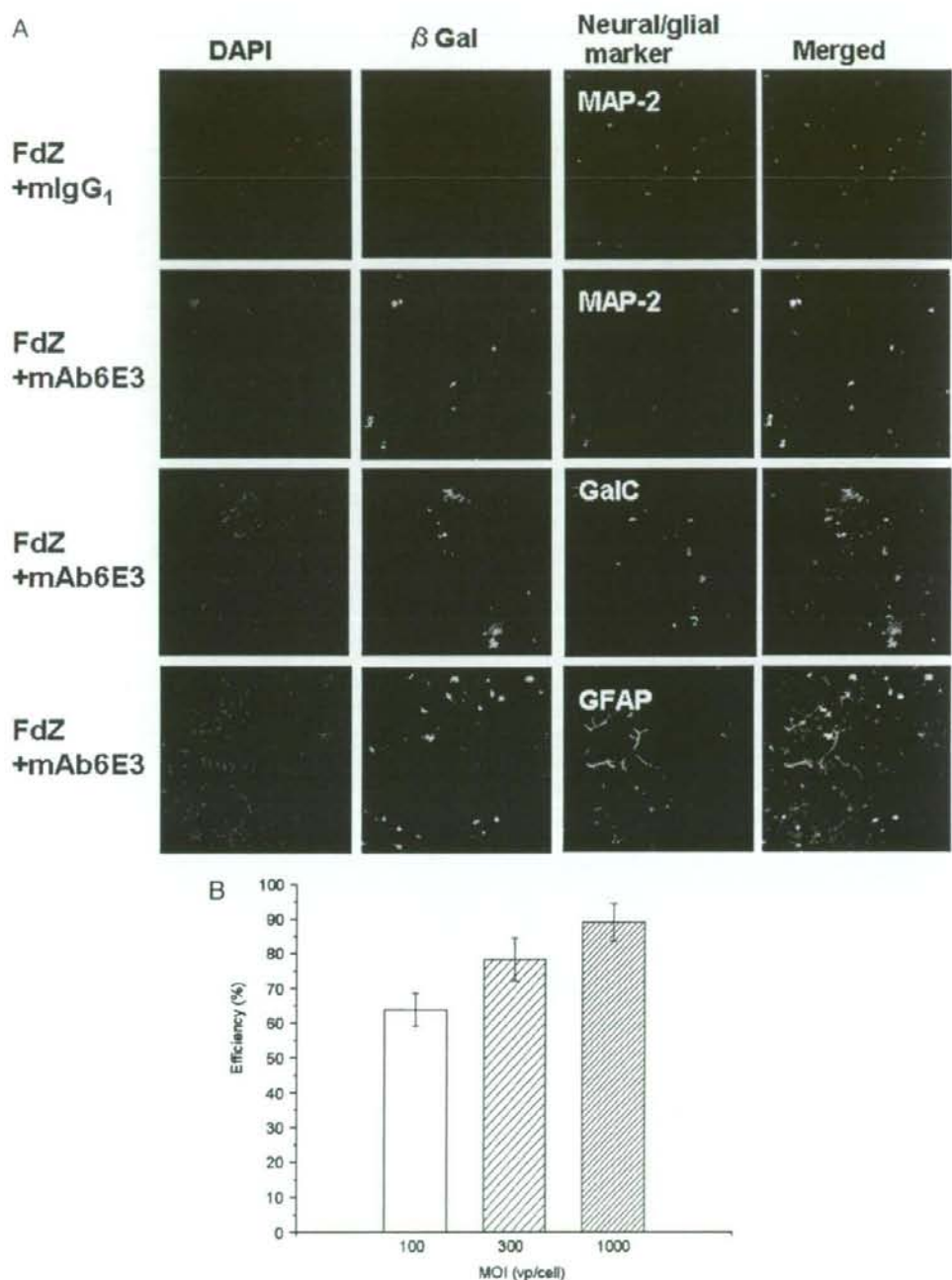


Figure 4. *In vitro* gene transfer into neuron–glia cocultures. (A) Immunofluorescent image at the MOI of 300. Cocultured neural cells were treated with adenovirus vectors (AdvZ3-FZ33 or AdvZ3-FdZ) and mAbs (control mIgG₁ or mAb6E3). Then, they were immunolabeled with anti- β -Gal mAb (green) and antibodies for neural markers (red; MAP2, GalC and GFAP). DAPI (blue) was used for counterstaining of the nuclei. (B) Quantification of gene transfer efficiency into the primary neuron. The number of β -Gal-positive neurons was counted at random in three selected fields and expressed as a percentage of all neurons at the fields

RNA interference transfection

PC12 cells were transfected with rat Na,K-ATPases β 1-specific siRNAs (Qiagen Atp1b1 siRNA, catalog number

SI01490307 and SI01490314) or a negative control siRNA (Qiagen AllStars negative control siRNA, catalog number 1027280) using HiPerfect reagent (Qiagen). The transfection mixtures were prepared in total 100 μ l

containing 3 μ l of HiPerfect and siRNA (final 5 nM) in serum-free Opti-MEM medium. The transfection mixtures were then transferred to 24-well plate and overlaid with 0.5 ml of PC 12 cell suspension (10^5 /ml) in serum-containing medium. The cells were then placed at 37°C for the indicated times. The surface antigen recognized by mAb6E3 was measured by flow cytometry. Mean fluorescence intensity (MFI) ratios were calculated as MFI of the mAb6E3 divided by MFI of corresponding mIgG1 k (MOPC-21) isotype control. Experiments were carried out in triplicate. MFI ratio of transfectants were compared and statistically analysed by Student's *t*-test. $p < 0.05$ was considered statistically significant.

Results

Development of monoclonal antibody, 6E3, and targeted gene transfer

To develop mAbs suitable for neuron-cell specific gene transfer using FZ33 fiber-modified adenovirus vectors, we immunized PC12 cells in mice and screened hybridomas by β -Gal reporter gene assay. β -Gal activity reflects the transfer efficiency of β -Gal gene into the PC12 cells via the antigen recognized by the antibodies secreted from the hybridoma. We found that β -Gal activity of the 6E3 well was constantly higher than that of other wells in the repeated assays. Thus, we cloned the hybridomas from the 6E3 well by limiting dilution and established the hybridoma, 6E3, that secretes mAb6E3 of the IgG₁ kappa isotype.

Subsequently, we examined the effects of mAb6E3 in Adv-FZ33-mediated gene transfer into several cell lines. As shown in Figure 1A, the efficacy of EGFP gene transfer by Adv-FZ33, as defined by the EGFP activity of cells, increased dramatically in the PC12 cells when the cells were treated with both AdvEGFP-FZ33 and mAb6E3. Such increase in the gene transfer efficacy was also observed in the NRK kidney and MTHC-1 thymoma cell lines, but not in the C6 glioma cell line. Notably, there were approximately 15% of the EGFP activities in the PC12 cells even when the cells were treated with AdvEGFP-FZ33 alone or AdvEGFP-FZ33 with the control mouse IgG₁ (mIgG₁). These activities are likely mediated via endogenous CAR-binding domain in Adv-FZ33.

Figure 1B shows cell surface expression of the 6E3 antigen in these cell lines. In line with mAb6E3-targeted gene transfer efficacy, PC12, NRK and MTHC-1 cells, but not C6 cells, expressed the mAb6E3 antigen.

mAb6E3-targeted gene transfer via Adv-FdZ

To specifically target mAb6E3 in gene transfer, we generated FdZ type adenovirus (Adv-FdZ) that lacks a CAR-binding motif. Thus, Adv-FdZ predominantly uses the IgG-binding motif to incorporate into cells. Figure 2

shows the efficacy of mAb6E3-targeted gene transfer into the PC12 cells via AdvZ3-FZ33 and AdvZ3-FdZ. As shown, AdvZ3-FZ33 transferred β -Gal gene into 5.2% of PC12 cells in the absence of mAb6E3, as defined by positive staining with anti- β -Gal mAb. This is probably due to the CAR-binding domain of AdvZ3-FZ33. By contrast, none of the PC12 cells treated with AdvZ3-FdZ and control mIgG₁ were positive for anti- β -Gal mAb. Notably, 40% of PC12 cells were stained positively with anti- β -Gal mAb when they were treated with both AdvZ3-FdZ and mAb6E3. These findings indicate the dependency of AdvZ3-FdZ-mediated gene transfer on mAb6E3.

In addition, we compared the capacity of AdvZ3-FZ33 and AdvZ3-FdZ in mediating mAb6E3-targeted gene transfer into the PC12 cells and C6 cells by chemiluminescent β -Gal reporter assays (Figure 3). In PC12 cells (Figure 3A), there was a linear correlation between β -Gal activity and viral concentration in all the experimental conditions, especially in those involving AdvZ3-FZ33. AdvZ3-FZ33 exhibited gene transfer efficacy, which was approximately five-fold higher in the conditions with mAb6E3 than in those without mAb6E3. By contrast, AdvZ3-FdZ showed approximately a 20-fold difference in gene transfer efficacy between the conditions in the presence and absence of mAb6E3. By contrast to PC12 cells, addition of mAb6E3 did not increase the gene transfer efficacy mediated by AdvZ3-FZ33 or AdvZ3-FdZ (Figure 3B) in C6 cells, indicating the dependency of gene transfer on the expression of the 6E3 antigen. The difference in gene transfer efficacy in the absence of mAb6E3 between PC12 and C6 cells likely reflects their distinct expression levels of integrins and CAR.

These findings are consistent with the structural characteristics of AdvZ3-FdZ that lacks the CAR-binding domain, thereby depending on IgG-binding domain for its gene transfer. Based upon these findings, we then focused on Adv-FdZ in the subsequent experiments.

Neuron-selective gene transfer in neuron-glia cocultures

Using Adv-FdZ, we examined whether mAb6E3-targeted gene transfer led to neuron-specific expression of the gene product. To address this *in vitro*, we used a kit composed of primary cultures from fetal rat cerebral cortex. The culture consists of three types of cells; neuron cells, oligodendrocytes, and astrocytes, as defined by the expression of specific markers MAP-2, GalC, and GFAP, respectively (Figure 4A). These mixed cell cultures were treated with AdvZ3-FdZ or a combination of AdvZ3-FdZ and mAb6E3. Figure 4A shows the immunofluorescent image at the MOI of 300. β -Gal gene was introduced into the cell culture by AdvZ3-FdZ depending on mAb6E3. Notably, the cells positive for anti- β -Gal mAb simultaneously were positive for anti-MAP-2 antibody. No such correspondence was observed in the expression of β -Gal and GalC or GFAP, indicating the specificity of mAb6E3-targeted gene transfer via Adv-FdZ into neuron

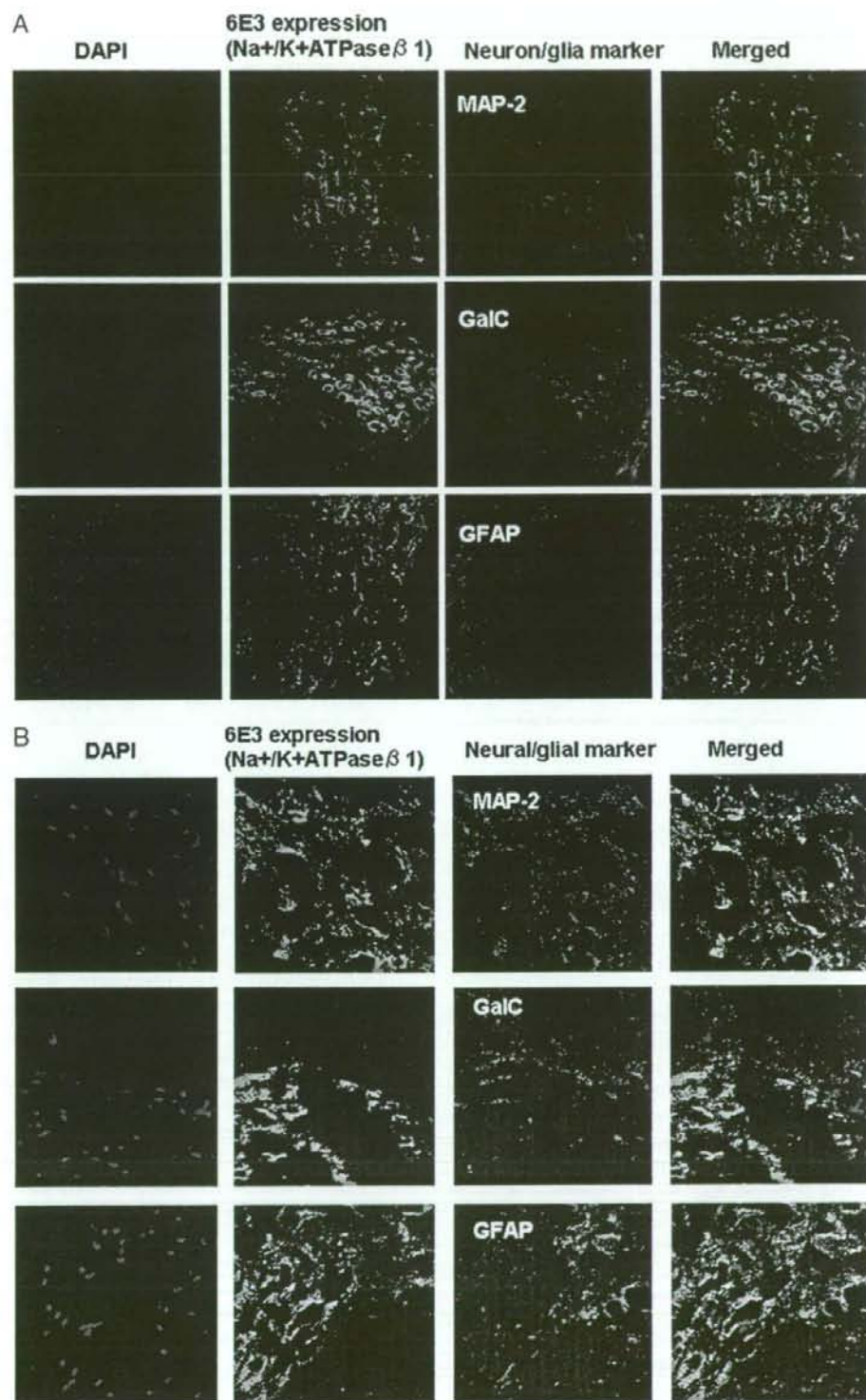


Figure 5. Immunostaining of rat spinal cord tissue with mAb6E3. (A) Representative images at low magnification ($\times 20$). (B) Representative images at high magnification ($\times 63$). Sections of rat spinal cord tissue were immunolabeled with mAb6E3 (green) and with antibodies for neural markers (red; MAP2, GalC and GFAP). DAPI (blue) was used for counterstaining. The expression of MAP-2 and Na₂K-ATPase β 1 was observed mainly in the gray matter, whereas GalC and GFAP were observed in the white matter

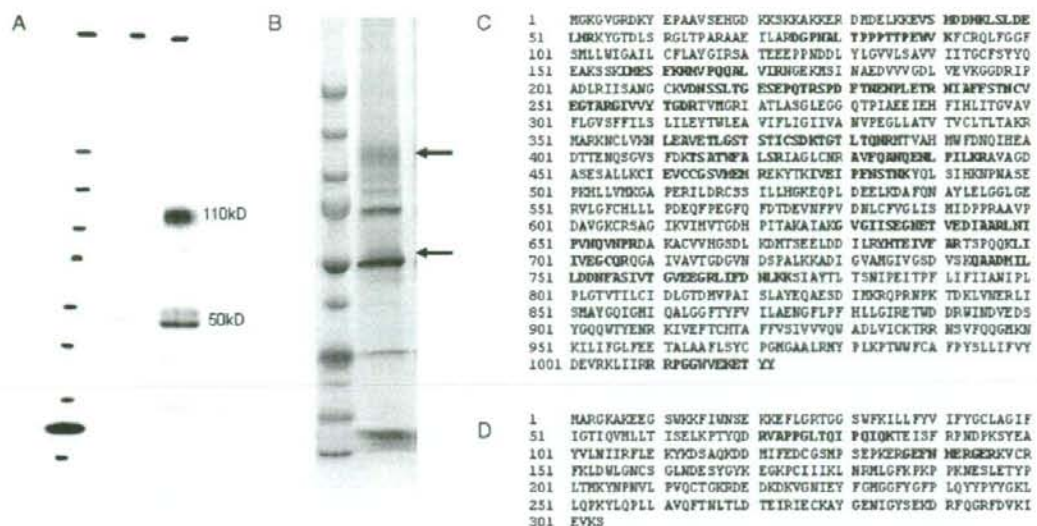


Figure 6. Identification of mAb6E3 antigen. (A) Immunoprecipitation of PC12 cell lysate with mAb6E3. Lysates of PC12 cells were immunoprecipitated with control mIgG₁ (left lane) and mAb6E3 (right lane). In the right lane, biotinylated proteins were immunoprecipitated at the molecular weight of 110- and 50-kDa. (B) Silver staining of PC12 cell lysate. PC12 cell lysate was immunoprecipitated with mAb6E3 on SDS/PAGE and then silver stained. From the silver-stained gel, two bands at 110- and 50-kDa (indicated by arrows) were excised from the gel and analysed by mass spectrometry, respectively. (C) Mass spectrometry of the 110-kDa protein. A band at 110 kDa was extracted from the gel, digested by trypsin, and analysed by oMALDI-Qq-TOF MS/MS QSTAR Pulsar. Figure 6C indicates the amino acid sequence of Na₂K-ATPase α 1. The sequence of the peptide detected from the 110-kDa protein band is indicated in bold. (D) Mass spectrometry of the 50-kDa protein. Similar to the 110-kDa protein band, the 50-kDa protein band was analysed. Figure 6D indicates the amino acid sequence of Na₂K-ATPase β 1. The sequence of the peptide detected from the 50-kDa protein band is indicated in bold

cells. The efficacy of neuron-selective gene transfer by a combination of AdvZ3-FdZ and mAb6E3 was in the range 65–90% in a dose-dependent manner (Figure 4B).

Distribution of mAb6E3 antigen in rat spinal cord

To determine whether mAb6E3 is useful for neuron-selective gene transfer *in vivo*, we stained rat spinal cord tissue with mAb6E3 and a specific marker of neural cells. Low magnification images (Figure 5A) showed the reactivity of mAb6E3 and anti-MAP-2 antibody (a specific marker of neurons) in the gray matter. By sharp contrast, GalC (a specific marker of oligodendrocytes) and GFAP (a specific marker of astrocytes) are expressed mainly in the white matter. The high magnification images (Figure 5B) show that the distribution of the cells reacting with mAb6E3 corresponds with the distribution of MAP-2-expressing cells, but not with GalC- or GFAP-expressing cells. These findings indicate that mAb6E3 react specifically with neuron cells in the neural tissue.

Identification of mAb6E3 antigen

Subsequently, we identified the antigen recognized by mAb6E3. As shown in Figure 6A, mAb6E3 immunoprecipitated 110- and 50-kDa proteins from the PC12 cell lysates. In western blot analysis with the PC12 lysate, mAb6E3

failed to detect any proteins (data not shown). Silver stain of SDS/PAGE where PC12 lysate had been immunoprecipitated with mAb6E3 revealed several protein bands, including two bands defined by immunoprecipitation using mAb6E3 (Figure 6B). The 110- and 50-kDa protein were cut and analysed by mass spectrometry. This analysis identified the extracted protein bands as rat Na₂K-ATPase α 1 and β 1, respectively (Figures 6C and 6D).

Na₂K-ATPase has three subunits (α , β and γ) that usually form complexes. The α subunit has 1–4 isoforms, the β subunit has 1–3 isoforms [25,26], and the γ subunit has three splice variants including variant a [27], b [28] and another [29] that we named c in the present study. To determine the antigen recognized by mAb6E3, we transfected each cDNA of these subunits and isoforms into 293T cells and assessed the reactivity of these transfectants with mAb6E3. As shown in Figure 7A, mAb6E3 did not cross-react with human cell-derived 293T cells (NT and pTarget). Among ten transfectants, mAb6E3 reacted only with the 293T transfectant expressing the Na₂K-ATPase β 1 subunit.

To further confirm the specificity of mAb6E3 to Na₂K-ATPase β 1 subunit, we carried out RNA interference transfection experiments using siRNAs specific to Na₂K-ATPase β 1 subunit. As shown in Figure 7B, transfection of PC12 with Atp1b1 (1) siRNA and Atp1b1 (2) siRNA resulted in significant decreases in the reactivity of PC12 with mAb6E3 as compared to PC12 cells transfected with a control siRNA.

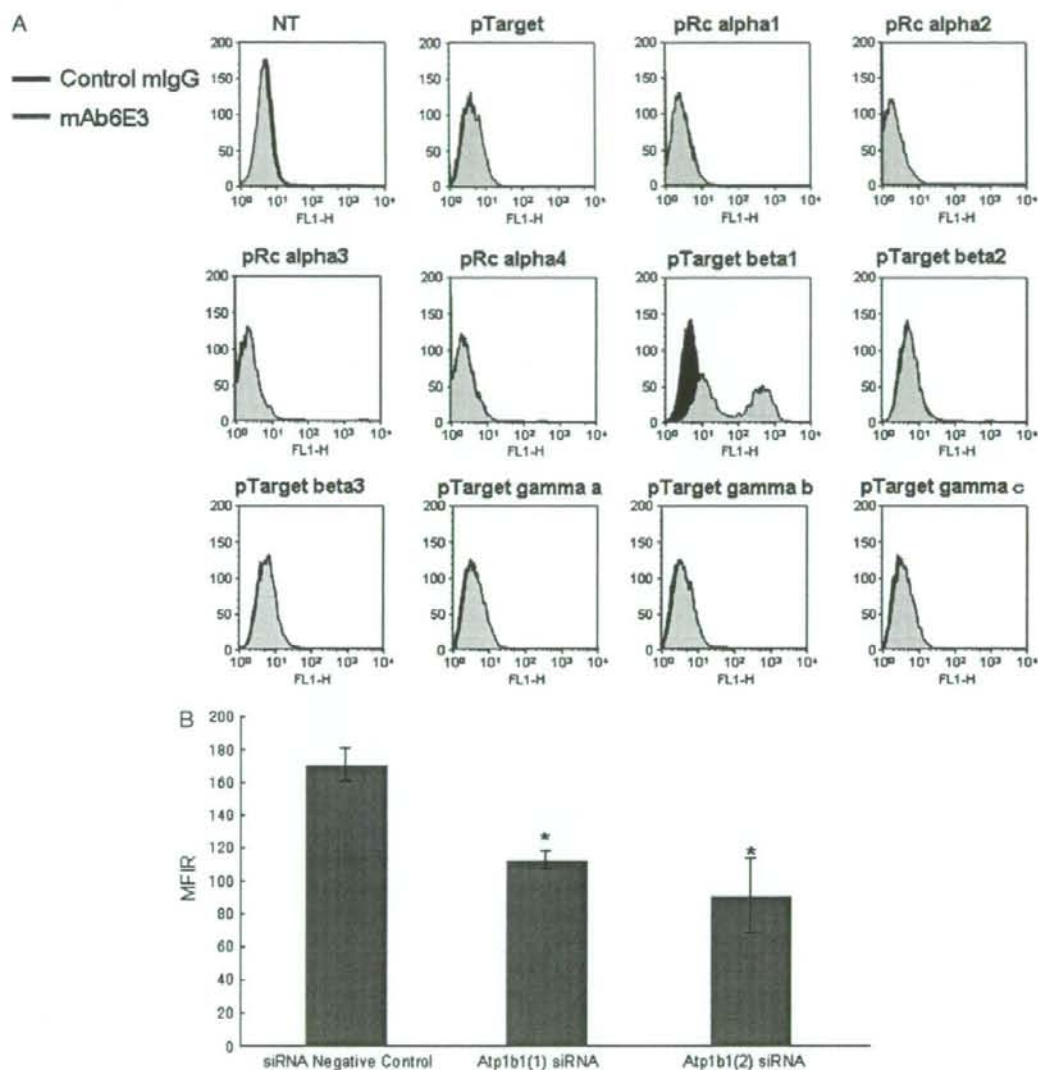


Figure 7. Transfection analysis of 6E3 antigen. (A) Reactivity of mAb6E3 with 293T cells transfected with cDNA of each subunit and isoform of rat Na,K-ATPase. The x-axis indicates the intensity of fluorescein isothiocyanate (FITC)-labeled cell surface molecule. The y-axis indicates cell counts. The 293T human cell line was transfected with each cDNA of ten isoforms and variants of Na,K-ATPase. mAb6E3 only reacted with 293T cells transfected with cDNA of rat Na,K-ATPase β 1. NT, no treatment; pTarget, transfectants of pTarget vector; pRc alpha 1–4, transfectants of 1–4 isoforms of the α subunit; pTarget beta 1–3, transfectants of 1–3 isoforms of the β subunit; pTarget gamma a–c, transfectants of a–c variants of the γ subunit. (B) Reactivity of mAb6E3 with PC12 cells transfected with siRNAs of rat Na,K-ATPase. PC12 were transfected with rat Na,K-ATPases β 1-specific siRNAs or a negative control siRNA using HiPerfect. The surface antigen recognized by mAb6E3 level were measured by flow cytometry. Expression levels were calculated as mean fluorescence intensity ratio and statistically analysed by Student's *t*-test. **p* < 0.05 compared to control siRNA.

Discussion

The primal requirements for successful gene therapy include: (i) abundant expression of target molecules on the cell surface of target cells; (ii) incorporation of the gene into the target cell; and (iii) expression of the gene products. Our hybridoma screening procedure is designed to quantitatively evaluate these requirements. Through the first screening by β -Gal reporter gene assay, we were

able to efficiently assess the efficacy of mAb-targeted gene transfer via fiber-modified adenovirus vectors. The subsequent screening focused on the specificity of mAb-targeted gene transfer and the identification of antigens recognized by the mAb. As a result of these screening procedures, we developed the hybridoma 6E3 and identified Na,K-ATPase β 1 as the antigen.

The immunostaining and chemiluminescent β -Gal reporter assays revealed that the mAb-targeted pathway

showed dose-dependent increases that were the same as the CAR-dependent pathway in gene transfer. These findings indicate that Na,K-ATPase β 1 functions the same as CAR as a target of gene transfer.

The Na,K-ATPase β 1 subunit has been shown to play a fundamental role in K^+ transport [30] and is distributed in almost all organs, especially in the brain and kidney [31]. Thus, Na,K-ATPase β 1 is not a neuron-specific molecule. However, previous reports [32–36] showed that Na,K-ATPase β 1 is expressed abundantly on the surface of neurons but poorly expressed on other types of neural cells, such as oligodendrocytes and astrocytes. Consistent with this, we found that the expression of Na,K-ATPase β 1 corresponded with that of MAP-2 but not with that of GalC or GFAP in the rat spinal cord tissue. In addition, mAb6E3-targeted gene transfer was specific to neuron cells in primary cultures of fetal rat cerebral cortex. The efficacy of mAb6E3-targeted gene transfer was in the range 65–90% depending on the virus doses. Since Cameron et al. [34] reported that the expression of Na,K-ATPase β 1 in immature neurons is lower than that of mature neurons, more efficient and selective gene transfer would perhaps be possible in mature neural tissue. Therefore, it is conceivable that Na,K-ATPase β 1 is a neuron-specific molecule in the neural tissues where it may serve as a target for neuron-specific gene transfer. Identification of an optimal ratio of antibodies to viruses as well as the development of new vectors superior to adenovirus are prerequisites for *in vivo* gene transfer.

In terms of clinical relevance, targeting of the Na,K-ATPase β 1 subunit may have adverse effects on cells since it plays a fundamental role in K^+ transport. In this regard, mAb6E3 did not affect the viability or form of the PC12 cells (data not shown). Neuron-specific expression of Na,K-ATPase β 1 in the neural tissues prefers the use of a mAb6E3-targeted gene transfer approach in local neurological disorders. In this regard, Agrawal and Fehlings [37] reported that Na,K-ATPase was involved in the mechanism of secondary spinal cord injury. Thus, gene transfer via Na,K-ATPase β 1 may target neurons that are secondarily injured.

Clearly, further studies including animal treatment models are necessary to demonstrate the feasibility of therapeutic targeting of transgene expression to neurons using mAb6E3 and AdvZ3-FdZ. For clinical application, it is also important to determine whether mAb6E3-targeted gene transfer can circumvent immunological reactions to adenovirus vectors. However, there are some problems with respect to performing an *in vivo* study. For example, animal models for neural disorders and methods of administration are not yet established. These are the critical themes for us to overcome in our next study.

In conclusion, the present study has demonstrated that hybridoma screening using FZ33 fiber-modified adenovirus vectors serves as an efficient approach for detecting antigens in mAb-targeted gene transfer. This approach may be more broadly applicable to other research fields. Na,K-ATPase β 1 defined by mAb6E3

represents a candidate molecule for neuron-selective gene transfer within the neural tissues.

Acknowledgements

We would like to thank Hiroshi Isogai and Noriko Kawano for their help with the animal experiments, Misumi Matsuo for her technical assistance and Dr Lingrel for providing the cDNAs. This work was supported in part by grants from the Japan Ministry of Education and Science, and by a grant from The General Insurance Association of Japan (03-25).

References

1. Fleischer A, Ghadiri A, Dessauge F, et al. Modulating apoptosis as a target for effective therapy. *Mol Immunol* 2006; **43**: 1065–1079.
2. Kennedy PG. Potential use of herpes simplex virus (HSV) vectors for gene therapy of neurological disorders. *Brain* 1997; **120**: 1245–1259.
3. Suwelack D, Hurtado-Lorenzo A, Millan E, et al. Neuronal expression of the transcription factor Gli1 using the T alpha1 alpha-tubulin promoter is neuroprotective in an experimental model of Parkinson's disease. *Gene Ther* 2004; **11**: 1742–1752.
4. Tuszynski MH, Hoi-Sang U, Alksne J, et al. Growth factor gene therapy for Alzheimer's disease. *Neurosci Focus* 2002; **13**: e5.
5. Hendriks WT, Ruitenberg MJ, Blits B, Boer GJ, Verhaagen J. Viral vector-mediated gene transfer of neurotrophins to promote regeneration of the injured spinal cord. *Prog Brain Res* 2004; **146**: 451–476.
6. Kurozumi K, Nakamura K, Tamiya T, et al. Mesenchymal stem cells that produce neurotrophic factors reduce ischemic damage in the rat middle cerebral artery occlusion model. *Mol Ther* 2005; **11**: 96–104.
7. Klein SM, Behrstock S, McHugh J, et al. GDNF delivery using human neural progenitor cells in a rat model of ALS. *Hum Gene Ther* 2005; **16**: 509–521.
8. Beck C, Uramoto H, Boren J, Akyurek LM. Tissue-specific targeting for cardiovascular gene transfer. Potential vectors and future challenges. *Curr Gene Ther* 2004; **4**: 457–467.
9. Kojima A, Tator CH. Intrathecal administration of epidermal growth factor and fibroblast growth factor 2 promotes ependymal proliferation and functional recovery after spinal cord injury in adult rats. *J Neurotrauma* 2002; **19**: 223–238.
10. Klimaschewski L, Nindl W, Feurle J, Kavakebi P, Kostrom H. Basic fibroblast growth factor isoforms promote axonal elongation and branching of adult sensory neurons *in vitro*. *Neuroscience* 2004; **126**: 347–353.
11. Ye J, Cao L, Cui R, et al. The effects of ciliary neurotrophic factor on neurological function and glial activity following contusive spinal cord injury in the rats. *Brain Res* 2004; **997**: 30–39.
12. Steffens S, Sandquist A, Frank S, et al. A neuroblastoma-selective suicide gene therapy approach using the tyrosine hydroxylase promoter. *Pediatr Res* 2004; **56**: 268–277.
13. Huang D, Desbois A, Hou ST. A novel adenoviral vector which mediates hypoxia-inducible gene expression selectively in neurons. *Gene Ther* 2005; **12**: 1369–1376.
14. Yano L, Shimura M, Taniguchi M, et al. Improved gene transfer to neuroblastoma cells by a monoclonal antibody targeting RET, a receptor tyrosine kinase. *Hum Gene Ther* 2000; **11**: 995–1004.
15. Gwag BJ, Kim EY, Ryu BR, et al. A neuron-specific gene transfer by a recombinant defective Sindbis virus. *Brain Res Mol Brain Res* 1998; **63**: 53–61.
16. Volpers C, Thirion C, Biermann V, et al. Antibody-mediated targeting of an adenovirus vector modified to contain a synthetic immunoglobulin γ -binding domain in the capsid. *J Virol* 2003; **77**: 2093–2104.
17. Roelvink PW, Mi Lee G, Einfeld DA, Kovessi I, Wickham TJ. Identification of a conserved receptor-binding site on the fiber proteins of CAR-recognizing adenoviridae. *Science* 1999; **286**: 1568–1571.

18. Kirby I, Davison E, Beavil AJ, et al. Mutations in the DG loop of adenovirus type 5 fiber knob protein abolish high-affinity binding to its cellular receptor CAR. *J Virol* 1999; **73**: 9508–9514.
19. Mizuguchi H, Koizumi N, Hosono T, et al. CAR- or alpha integrin-binding ablated adenovirus vectors, but not fiber-modified vectors containing RGD peptide, do not change the systemic gene transfer properties in mice. *Gene Ther* 2004; **9**: 769–776.
20. Tanaka T, Huang J, Hirai S, et al. Carcinoembryonic antigen-targeted selective gene therapy for gastric cancer through FZ33 fiber-modified adenovirus vectors. *Clin Cancer Res* 2006; **12**: 3803–3813.
21. Nakamura T, Sato K, Hamada H. Effective gene transfer to human melanomas via integrin-targeted adenoviral vectors. *Hum Gene Ther* 2002; **13**: 613–626.
22. Nyberg-Hoffman C, Shabram P, Li W, Giroux D, Aguilar-Cordova E. Sensitivity and reproducibility in adenoviral infectious titer determination. *Nat Med* 1997; **3**: 808–811.
23. Zhang WW, Koch PE, Roth JA. Detection of wild-type contamination in a recombinant adenoviral preparation by PCR. *Biotechniques* 1995; **18**: 444–447.
24. Uchida H, Shinoura N, Kitayama J, Watanabe T, Nagawa H, Hamada H. 5-Fluorouracil efficiently enhanced apoptosis induced by adenovirus-mediated transfer of caspase-8 in DLD-1 colon cancer cells. *J Gene Med* 2003; **5**: 287–299.
25. Woo AL, James PF, Lingrel JB. Characterization of the fourth alpha isoform of the Na, K-ATPase. *J Membr Biol* 1999; **169**: 39–44.
26. Kuster B, Shainskaya A, Pu HX, et al. A new variant of the gamma subunit of renal Na, K-ATPase. Identification by mass spectrometry, antibody binding, and expression in cultured cells. *J Biol Chem* 2000; **16**: 18441–18446.
27. Therien AG, Karlish SJ, Blostein R. Expression and functional role of the gamma subunit of the Na, K-ATPase in mammalian cells. *J Biol Chem* 1999; **274**: 12252–12256.
28. Arystarkhova E, Wetzel RK, Sweadner KJ. Distribution and oligomeric association of splice forms of Na(+)-K(+)-ATPase regulatory gamma-subunit in rat kidney. *Am J Physiol Renal Physiol* 2002; **282**: F393–F407.
29. Mercer RW, Biemesderfer D, Bliss DP Jr, Collins JH, Forbush B III. Molecular cloning and immunological characterization of the gamma polypeptide, a small protein associated with the Na, K-ATPase. *J Cell Biol* 1993; **121**: 579–586.
30. Agrawal SK, Fehlings MG. Mechanisms of secondary injury to spinal cord axons *in vitro*: role of Na⁺, Na(+)-K(+)-ATPase, the Na(+)-H⁺ exchanger, and the Na(+)-Ca²⁺ exchanger. *J Neurosci* 1996; **16**: 545–552.
31. Geering K. The functional role of beta subunits in oligomeric P-type ATPases. *J Bioenerg Biomembr* 2001; **33**: 425–438.
32. Watts AG, Sanchez-Watts G, Emanuel JR, Levenson R. Cell-specific expression of mRNAs encoding Na⁺, K(+)-ATPase alpha- and beta-subunit isoforms within the rat central nervous system. *Proc Natl Acad Sci USA* 1991; **88**: 7425–7429.
33. Cameron R, Klein L, Shyjan AW, Rakic P, Levenson R. Neurons and astroglia express distinct subsets of Na, K-ATPase alpha and beta subunits. *Brain Res Mol Brain Res* 1994; **21**: 333–343.
34. Peng L, Martin-Vasallo P, Sweadner KJ. Isoforms of Na, K-ATPase alpha and beta subunits in the rat cerebellum and in granule cell cultures. *J Neurosci* 1997; **17**: 3488–3502.
35. Peng L, Arystarkhova E, Sweadner KJ. Plasticity of Na, K-ATPase isoform expression in cultures of flat astrocytes: species differences in gene expression. *Glia* 1998; **24**: 257–271.
36. Martin-Vasallo P. Oligodendrocytes in brain and optic nerve express the beta3 subunit isoform of Na, K-ATPase. *Glia* 2000; **31**: 206–218.
37. Blaneo G, Mercer RW. Isozymes of the Na-K-ATPase: heterogeneity in structure, diversity in function. *Am J Physiol* 1998; **275**: F633–F650.